

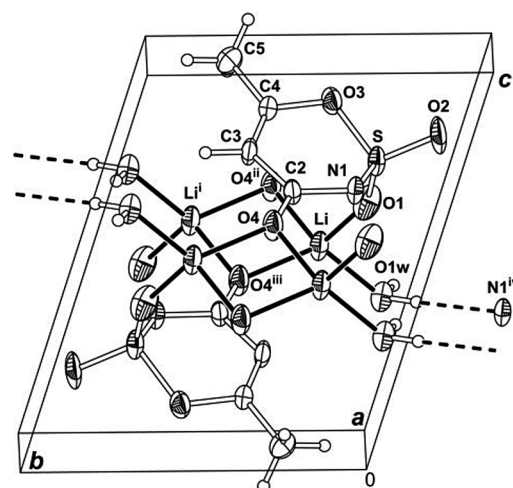
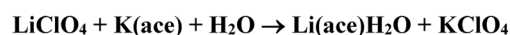
Structural and IR-Spectroscopic Characterization of Aqua Lithium Acesulfamate, an Outlier of the M(ace), M: Na⁺, K⁺, Rb⁺, Cs⁺, Isomorphic Series

Oscar E. Piro¹ · Gustavo A. Echeverría¹ · Beatriz S. Parajón-Costa² · Enrique J. Baran²

Received: 26 September 2017 / Accepted: 14 October 2017 / Published online: 25 October 2017
 © Springer Science+Business Media, LLC 2017

Abstract The crystal structure of aqua lithium 6-methyl-1,2,3-oxathiazine-4(3H)-one, 2,2-dioxide, for short Li(ace)H₂O, was determined by X-ray diffraction methods. It crystallizes in the triclinic P $\bar{1}$ space group with $a = 6.1750(9)$ Å, $b = 7.3969(9)$ Å, $c = 9.016(1)$ Å, $\alpha = 105.88(1)^\circ$, $\beta = 94.59(1)^\circ$, $\gamma = 97.80(1)^\circ$, and $Z = 2$ molecules per unit cell. The crystal structure of Li(ace)H₂O sharply departs from the other heavier alkaline-metal acesulfamates, namely the monoclinic isotypic M-ace (M from Na⁺ to Cs⁺) family of salts. Lithium is in a distorted LiO₄ tetrahedral coordination with acesulfamate carbonyl, sulfoxide and water oxygen atoms. The FTIR spectrum of the new compound was also recorded and is briefly discussed. Some comparisons with other simple acesulfamate salts are also made.

Graphical Abstract The synthesis of aqua lithium acesulfamate, Li(C₄H₄NO₄S)H₂O, and its structural characterization by single-crystal X-ray diffractometry are reported. The FTIR spectrum of the salt is analyzed by comparison with data of related compounds.



Keywords Aqua lithium acesulfamate · Synthesis · Crystal structure · FTIR spectrum

Introduction

Acesulfame-K, the potassium salt of 6-methyl-1,2,3-oxathiazin-4(3H)-one-2,2-dioxide (Fig. 1), is one of the most widely used non-caloric artificial sweeteners [1, 2]. Its general chemical and biological properties have been thoroughly investigated [3, 4], and its crystal structure has also been determined [5].

From the chemical and structural points of view, the acesulfamate anion bears some resemblance to saccharin (1,2-benzothiazole-3(2H)-one-1,1-dioxide), whose coordination capacity has been intensively exploited during the

CIF has been deposited at the Cambridge Crystallographic Data Center, Reference Number CCDC 1574391.

✉ Enrique J. Baran
 baran@quimica.unlp.edu.ar

¹ Departamento de Física and Instituto IFLP (CONICET-CCT-La Plata), Facultad de Ciencias Exactas, Universidad Nacional de La Plata, 1900 La Plata, Argentina

² Centro de Química Inorgánica (CEQUINOR/CONICET-CCT-La Plata, UNLP), Facultad de Ciencias Exactas, Universidad Nacional de La Plata, Bvd. 120, N 1465, 1900 La Plata, Argentina

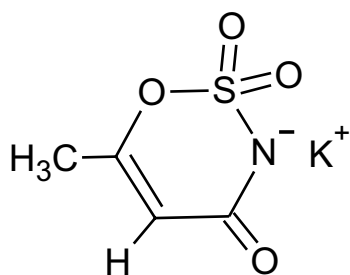


Fig. 1 Schematic structure of potassium acesulfamate

last years (for a recent review *cf.* [6]). Similarly to saccharinate, the acesulfamate anion presents different potential coordination sites (the imine nitrogen, the carbonyl oxygen and the two sulfonyl oxygen atoms) and it can act as a mono-dentate, bi-dentate or bridging ligand. This versatility has been widely exploited and numerous metal complexes containing the acesulfamate ligand have been reported and characterized during the last years (*cf.* for example [7] and references therein).

Notwithstanding, simple salts of this anion have only been prepared and characterized most recently [8–13]. In particular, we have found that all the alkaline metal cations from Na^+ to Cs^+ conforms an isotopic series (monoclinic, non-conventional space group $P2_1/a$, $Z = 4$) [10]. In order to complement the characterization of the acesulfamates of the alkali-metal series, we have now synthesized and investigated the corresponding lithium salt.

Besides, the chemistry of lithium is very interesting on its own and has awaked great expectations during the last years, due to its important and varied technological applications [14–16]. It is the most electropositive metal, the lightest and least dense solid element at room temperature and is a very reactive element. These peculiar physical, chemical and electrochemical properties make lithium and some of its compounds very attractive to many fields. Apart from the recent advent of lithium-based batteries, which is responsible for the major present interest in this element, some other applications and uses are also very important and interesting. Lithium compounds are used in glass and ceramic manufacture, as well as additives in Portland and high-alumina cements. Some of its organometallic compounds are important industrial catalysts and as a reducing agent (in the form of LiH and LiAlH_4) it is used in the synthesis of a lot of fine chemicals of pharmaceutical and agrochemical interest. As LiF or Li_2CO_3 it is employed to lowering the melting point of the cryolite bath in the aluminum production, and other of its compounds (LiBr or LiCl) are used in air conditioning systems. The Li/Al and Li/Mg systems are the basis of the so-known “light alloys” used in the aeronautical, aerospace and automotive industries. The addition of lithium compounds as thickening agents in lubricating

greases caused a profound impact in the field of tribology during the last years and one particular compound, lithium niobate, LiNbO_3 , appeared as an important novel material in nonlinear optics. Lithium also occupies a central place in modern nuclear technology, as ^3H is obtained by neutron irradiation of ^6Li and both natural lithium isotopes (^6Li and ^7Li) are increasingly employed in nuclear reactors. Finally, the effect of some simple lithium salts on the nervous system has also made lithium attractive as a mood-stabilizing drug and some of its compounds have recently shown other types of pharmacological activity [16].

Experimental

Materials and Measurements

Potassium acesulfamate was supplied by Fluka, lithium carbonate by Sigma, whereas all the other employed reagents were from Merck, analytical grade, and were used as purchased. Elemental analysis of the compounds was performed with a Carlo Erba model EA 1108 elemental analyzer. The infrared spectra were recorded on a FTIR-Bruker-EQUINOX-55 spectrophotometer (resolution 4 cm^{-1}) in the spectral range between 4000 and 400 cm^{-1} , using the KBr pellet technique.

Synthesis of the Compound

Initially we have attempted to obtain lithium acesulfamate, using the same general methodology employed in our previous studies, *i.e.* reaction between aqueous solutions of acesulfamic acid (prepared from potassium acesulfamate, following the procedure of Velaga *et al.* [17]) and Li_2CO_3 [9–11, 13]. The crystalline solid, collected after the evaporation of the solution during a few days, results pure acesulfamic acid, showing that no interaction occurred.

Therefore, we have applied an alternative synthetic procedure, based on the reaction of lithium perchlorate with potassium acesulfamate [8, 12], which we have also previously employed successfully for the preparation of sodium acesulfamate [10], working in the following way: To 1.00 g of Li_2CO_3 suspended in 10 mL of distilled water at $85\text{ }^\circ\text{C}$, the equivalent amount of concentrated HClO_4 (*ca.* 2.6 mL) was dropwise added under continuous stirring. To the generated lithium perchlorate solution, 10 mL of a hot aqueous solution ($85\text{ }^\circ\text{C}$) containing 5.44 g of potassium acesulfamate was dropwise added. Stirring at $85\text{ }^\circ\text{C}$ was maintained for further 30 min more. The solution was cooled down to room temperature and then left in a freezer ($-5\text{ }^\circ\text{C}$) during half an hour. The precipitated KClO_4 was separated from the cold solution by filtration and the remaining solution was left to evaporate in air. After some days well-formed colorless

crystals were deposited. The purity of the obtained salt was confirmed by elemental analysis. $C_4H_6LiNO_5S$ (187.10): calcd. C 25.67, H 3.23, N 7.48, S 17.14%; found C 25.60, H 3.27, N 7.45, S 17.10%.

Single crystals adequate for structural X-ray diffraction studies were selected from the crystalline mass employing a microscope.

Caution

Please, remember that $HClO_4$ is a strong mineral acid which, under some circumstances, may act as an oxidizer and/or present explosion hazards. Organic materials are especially susceptible to spontaneous combustion if contacted with the acid. The acid may cause eye damage and skin burns.

Single Crystal X-ray Diffraction

The X-ray diffraction experiments were performed on an Oxford Xcalibur, Eos, Gemini CCD diffractometer, employing graphite-monochromated $MoK\alpha$ ($\lambda = 0.71073 \text{ \AA}$) radiation. X-ray diffraction intensities were collected (ω scans with ϑ and κ -offsets), integrated and scaled with CrysAlis-Pro [18] suite of programs. The unit cell parameters were obtained by least-squares refinement (based on the angular settings for all collected reflections with intensities larger than seven times the standard deviation of measurement errors) using CrysAlisPro. Data were corrected empirically for absorption with the multi-scan method implemented in CrysAlisPro.

The structure was solved by intrinsic phasing with SHELXT of the SHELX suit of programs [19] and refined by least-squares with SHELXL of the same package. All hydrogen atoms were determined in a Fourier difference map phased on the heavier atoms. However, the acesulfamate methyl hydrogen atoms were refined with the riding model and their locations optimized during the refinement by treating them as rigid bodies which were allowed to rotate around the corresponding C–CH₃ bond such as maximize the residual electron density at their calculated positions. As a result, the methyl groups converged to staggered angular conformations. The acesulfamate aromatic and water H-atoms were refined at their found position with isotropic displacement parameters and Ow–H and H \cdots H distances restrained to target values of 0.86(1) and 1.36(1) Å, respectively. Crystal data and refinement results are summarized in Table 1.

Powder X-ray Diffraction (PXRD)

The PXRD pattern of $Li(ace)H_2O$ was obtained with a Phillips PW-1710 diffractometer, using $CuK\alpha$ radiation ($\lambda = 1.5406 \text{ \AA}$) from an X-ray tube operated at 35 kV and

Table 1 Basic crystallographic data, data collection and refinement results of $Li(ace)H_2O$

Empirical formula	$C_4H_6LiNO_5S$
Formula weight	187.10
Temperature (K)	297 (2)
Crystal size, mm ³	0.329 × 0.194 × 0.058
Crystal shape and color	Plate, colorless
Crystal system	Triclinic
Space group	$P\bar{1}$
<i>a</i> (Å)	6.1750 (9)
<i>b</i> (Å)	7.3969 (9)
<i>c</i> (Å)	9.016 (1)
α (°)	105.88 (1)
β (°)	94.59 (1)
γ (°)	97.80 (1)
<i>V</i> (Å ³)	389.45 (9)
<i>Z</i>	2
D.c (g cm ⁻³)	1.596
Absorption coefficient (mm ⁻¹)	0.393
F(000)	192
θ (°)-range for data collection	2.903; 28.838
Index ranges	<i>h</i> (–8; 7) <i>k</i> (–9; 9) <i>l</i> (–11; 7)
Reflections measured/unique/observed	2901/1669/1195
Refinement method	Full-matrix least-squares on F ²
Data/restraints/parameters	1669/3/122
Goodness of fit on F ²	1.046
R1/wR2 [<i>I</i> > 2 σ (<i>I</i>)]	0.0616/0.1487
R1/wR2 (all data)	0.0876/0.1785
Largest differ. peak and hole (e Å ⁻³)	0.448; –0.422
CIF-file deposition number	CCDC 1574391

30 mA. The X-ray diffraction patterns were collected in the $8^\circ \leq 2\theta \leq 48^\circ$ range, with 0.02° step width and 3.2 s counting time per step employing the Bragg–Brentano θ – 2θ geometry, a scintillation counter and an exit beam graphite monochromator.

Results and Discussion

Crystal Structure

An ORTEP [20] plot of the lithium salt is shown in Fig. 1 and corresponding bond distances and angles within the acesulfamate molecule and around the lithium ion are given in Tables 2 and 3, respectively. In sharp contrast with the rest of the alkali sulfamate salts, namely the isotypic M-ace (M: Na⁺, K⁺, Rb⁺, Cs⁺) series, where the alkali metal show

Table 2 Bond lengths (Å) and angles (°) of the acesulfamate anion in Li(ace)H₂O

C(2)–O(4)	1.244 (4)	N(1)–C(2)–C(3)	120.0 (3)
C(2)–N(1)	1.359 (4)	C(4)–C(3)–C(2)	123.4 (3)
C(2)–C(3)	1.453 (5)	C(3)–C(4)–O(3)	121.0 (3)
C(3)–C(4)	1.316 (5)	C(3)–C(4)–C(5)	128.2 (3)
C(4)–O(3)	1.387 (4)	O(3)–C(4)–C(5)	110.8 (3)
C(4)–C(5)	1.487 (5)	C(2)–N(1)–S	117.9 (2)
N(1)–S	1.554 (3)	C(4)–O(3)–S	116.4 (2)
O(1)–S	1.421 (3)	O(2)–S–O(1)	114.7 (2)
O(2)–S	1.419 (3)	O(2)–S–N(1)	111.2 (2)
O(3)–S	1.614 (3)	O(1)–S–N(1)	113.0 (2)
		O(2)–S–O(3)	104.5 (2)
O(4)–C(2)–N(1)	119.2 (3)	O(1)–S–O(3)	105.6 (2)
O(4)–C(2)–C(3)	120.7 (3)	N(1)–S–O(3)	107.1 (1)

Table 3 Short contacts (Å) and angles (°) around lithium in Li(ace)H₂O

Li–O(1W)	1.901(6)	O(1W)–Li–O(1)	102.6(3)
Li–O(1)	1.943(7)	O(1W)–Li–O(4)#1	119.3(3)
Li–O(4)#1	1.949(7)	O(1)–Li–O(4)#1	110.9(3)
Li–O(4)#2	1.957(6)	O(1W)–Li–O(4)#2	122.4(4)
		O(1)–Li–O(4)#2	113.6(3)
		O(4)#1–Li–O(4)#2	88.1(2)

Symmetry transformations used to generate equivalent atoms: (#1) $x+1, y, z$; (#2) $-x+1, -y+1, -z+1$

(up to a sphere of 3.5 Å radius) coordination numbers of five for sodium (NaNO₄ core) and eight for the larger sized potassium to cesium ions (MNO₇ core), the small ionic radius of lithium limits the number of ligand atoms in the metal coordination sphere before strong steric ligand–ligand repulsion effect (crowding) sets in. In fact, in Li(ace)H₂O the lithium ion is in a distorted tetrahedral environment (LiO₄ core) coordinated to one sulfoxide oxygen atom of an ace ligand [$d(\text{Li}–\text{O}) = 1.943(7)$ Å], to two carbonyl oxygen atoms, one from a neighboring, inversion-related, ace molecule [$d(\text{Li}–\text{O}) = 1.957(6)$ Å] and the other one belonging to another ligand molecule symmetry-related through a unit cell translation along the *a*-axis [$d(\text{Li}–\text{O}) = 1.949(7)$ Å]. This gives rise to a one-dimensional chain structure that extends along this axis (see Fig. 1). The fourth tetrahedral site is occupied by a water molecule [$d(\text{Li}–\text{Ow}) = 1.901(6)$ Å]. Tetrahedral lithium coordination with short Li–ligand bonds is also observed in lithium orotate monohydrate (LiO₄ core) where Li–O bond lengths are in the 1.882(3)–1.991(3) Å range [21], close to the one observed in the present case. On the other hand, crowding coordination effect leading to longer Li–ligand contact distances are observed for five-fold coordinated lithium in other organic salts, including lithium citrate monohydrate (distorted square pyramid LiO₅

core), where Li–O distances are in the 2.007(3)–2.089(3) Å range [22] and mono aqua lithium isoorotate (trigonal bipyramidal LiO₅ core) where Li–O distances are in the 2.010(3)–2.142(3) Å range [23].

Observed bond distances and angles of the acesulfamate ligand in Li(ace)H₂O salt agree with corresponding values reported for other related salts [9–11, 13]. Particularly, the short C3–C4 distance of 1.316(5) Å confirms the formal double bond character expected for this link. The carbonyl >C=O double bond distance is 1.244(4) Å and sulfoxide S=O distances are 1.421(3) and 1.419(3) Å. The other ring single bond lengths are $d(\text{C}–\text{O}) = 1.387(4)$ Å, $d(\text{O}–\text{S}) = 1.614(3)$ Å, $d(\text{S}–\text{N}) = 1.544(3)$ Å, $d(\text{C}–\text{N}) = 1.359(4)$ Å, and $d(\text{C}–\text{C}) = 1.453(5)$ Å. These bond lengths can be compared with those of the free solid acesulfamic acid molecule (triclinic P $\bar{1}$ space group) [17]. The main change in the bonding structure of the acesulfamate ion in the lithium salt occurs at the S–N bond, which upon deprotonation shortens in 0.075 Å (about 25 times the standard error σ). A much smaller shortening (-0.023 Å = -5.7σ) is observed in the N–C bond length. Other significant bond length changes when going from the acid to the acesulfamate anion are observed for the ring S–O and O–C bonds ($+0.021$ Å = $+7\sigma$ and -0.018 Å = -4.5σ , respectively).

Neighboring $\cdots\text{Li}(\text{ace})\text{H}_2\text{O}–\text{Li}(\text{ace})\text{H}_2\text{O}–\cdots$ chains, symmetry related through a unit-cell translations along the *b*-axis, are OwH \cdots N bonded to each other [$d(\text{OwH}\cdots\text{N}) = 2.19(1)$ Å; $\angle(\text{Ow}–\text{H}\cdots\text{N}) = 177(5)^\circ$], giving rise to a layered structure parallel to (001) plane, where adjacent layers are displaced in a unit-cell translation along the *c*-axis and bonded to each other through weak van der Waals interaction. This explains the observation that the crystals grow as thin plate parallel to (001), which is therefore an easy-cleavage crystal plane.

It is interesting to mention, that often structural relationships between acesulfamate complexes and salts, and the respective saccharinate compounds have been observed. In the present case, such a comparison is not possible as lithium saccharinate has so far not been characterized [6]. Another interesting comparison is that of Li(ace)(H₂O) with the corresponding Mg(II) acesulfamate, Mg(ace)·6H₂O, taking into account the well-known “diagonal relationship” between Li(I) and Mg(II) [24].

In the case of the magnesium salt, the Mg(II) cation is at a crystallographic inversion center in an octahedral environment of water molecules which are coordinated through their oxygen lone pairs. This prevents the Mg(II) ion from direct electrostatic interactions with the acesulfamate anion, as it happens in the now investigated lithium salt, and the ionic $[\text{Mg}(\text{H}_2\text{O})_6]^{2+}/\text{Ace}^-$ interaction is mediated by H-bonding [13].

Crystallographic structural data have been deposited at the Cambridge Crystallographic Data Centre (CCDC). Any

request to the Cambridge Crystallographic Data Centre for this material should quote the full literature citation and the reference number CCDC 1574391.

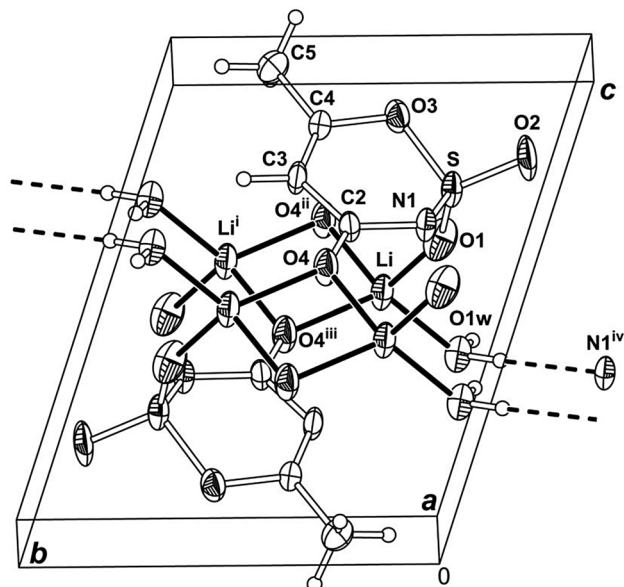
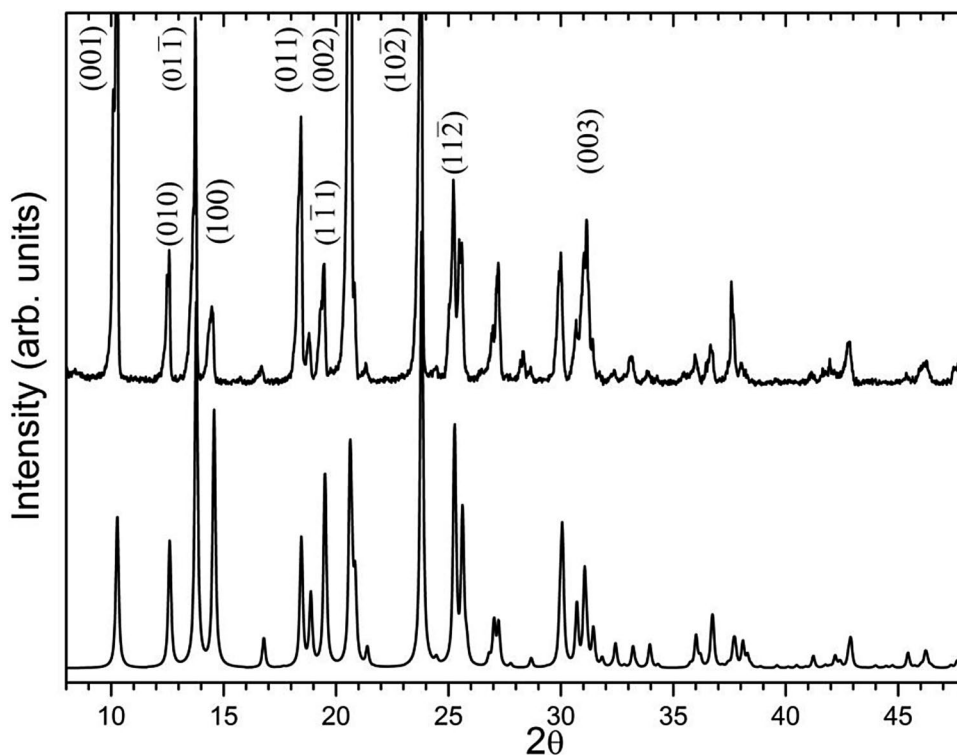


Fig. 2 Projection down the crystal a -axis of aqua lithium acesulfamate, showing the labeling of the non-H atoms and their displacement ellipsoids at the 30% probability level. Metal–ligand bonds are indicated by full lines and H-bonds by dashed lines. Crystal symmetry operations: (i) $2-x, 1-y, 1-z$; (ii) $1+x, y, z$; (iii) $1-x, 1-y, 1-z$; (iv) $1-x, -y, 1-z$

Fig. 3 Upper trace experimental PXRD pattern of aqua lithium acesulfamate, collected with $\text{CuK}\alpha$ radiation, showing the Miller indices of ten diagnostic lines. Lower trace PXRD pattern calculated from the crystal structure of $\text{Li}(\text{ace})\text{H}_2\text{O}$



Discussion of PXRD Data

In Fig. 2 we compare the powder X-ray diffraction patterns of $\text{Li}(\text{ace})\text{H}_2\text{O}$ salt with the calculated one [25] derived from the single crystal X-ray structure. The figure shows that the materials in the polycrystalline aggregation state employed in the spectroscopic study reported here has the same crystal structure as its single crystal counterpart without significant contribution of other crystalline phases.

Differences between experimental and theoretical integrated peaks intensities could be due in part to polycrystalline preferential orientation in the powder. The orientation effect is particularly notorious for the $(00l)$ reflections with $l = 1, 2, 3$ (see Fig. 3). This is due to preferred orientation along the crystal reciprocal c^* -axis of the powder when pressed onto the sample holder employed in the PXRD measurements. The orientation, in turn, is favored by the fact stated above that the crystals grow as thin crystal plate parallel to (001) plane.

It can be observed diagnostic powder diffraction peaks (Miller indexes in parentheses) at unique 2θ -values (in degrees) of 10.24 (001), 12.50 (010), 13.64 (01 $\bar{1}$), 14.45 (100), 18.33 (011), 19.25 (1 $\bar{1}$ 1), 20.61 (002), 23.66 (10 $\bar{2}$), 25.16 (11 $\bar{2}$) and 30.93 (003), with an estimated error of $\pm 0.03^\circ$.

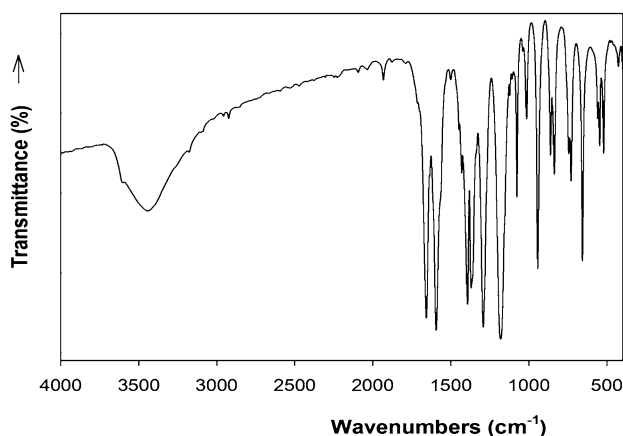


Fig. 4 FTIR spectrum of Li(ace)H₂O in the spectral range between 4000 and 400 cm⁻¹

Table 4 Assignment of the FTIR spectrum of aqua lithium acesulfamate^a

Band position (cm ⁻¹)	Proposed assignment
3622 vw, 3442 vs, br	$\nu(\text{OH}) (\text{H}_2\text{O})$
1657 vs, 1594 vs/1560 sh	$\nu(\text{C}=\text{O}) + \nu(\text{C}-\text{C})$ ring
1430 vw, 1392 vs	$\delta(\text{CH}_3)$
1370 vs	$\nu_{\text{as}}(\text{SO}_2)$
1292 vs	$\nu(\text{CN}) + \nu(\text{OC}) + \delta(\text{CCH})$
1180 vs	$\nu_{\text{s}}(\text{SO}_2) + \nu(\text{SN})$
1076 m	$\delta(\text{CH}_3)$
1040 vw/1014 m	$\nu(\text{OC}) + \nu(\text{SN})$
942 vs	$\nu(\text{OC}) + \nu(\text{C}-\text{CH}_3)$
861 m	$\tau(\text{ring})$
837 m	$\nu(\text{SN}) + \nu(\text{C}-\text{C}) + \delta(\text{NCO})$
744 w/728 m	$\tau(\text{ring})$
656 vs	$\delta(\text{ring})$
559 w/546 m	$\delta(\text{ring}) + \delta(\text{SO}_2)$
520 m	$\tau(\text{ring})$
425 m, br	$\rho_{\text{w}}(\text{H}_2\text{O}) + \tau(\text{ring})$

^avs very strong, *s* strong, *m* medium, *w* weak, *vw* very weak, *br* broad, *sh* shoulder

IR-Spectrum

The FTIR spectrum of Li(ace)H₂O shown in Fig. 4, is similar to those measured in the case of some of the previously investigated acesulfamate salts [10, 11, 13]. The spectral assignment, presented in Table 4, was performed on the basis of a recent experimental and DFT-study of potassium acesulfamate [26], additionally supported by our previous studies [9–11, 13], and is briefly discussed, as follows:

- The O–H stretching vibrations of the bonded water molecule generate a strong, relatively broad and well-defined band accompanied by a weak shoulder. The corresponding deformation mode, $\delta(\text{H}_2\text{O})$, is probably overlapped by bands found in the 1600–1660 cm⁻¹ region. From the spectroscopic point of view, the hydrogen bridges generated by this water molecule can be classified as H-bonds of medium strength [27, 28].
- IR bands related to the CH and CH₃ stretching modes, expected in the 2800–3200 cm⁻¹ range [29], are usually very weak and, accordingly, generate only a series of very weak IR signals in this region.
- As in the previously investigated cases, vibration modes related to $\nu(\text{C}=\text{O})$ and $\nu(\text{C}-\text{C})$ stretches are strongly coupled resulting in two of the most intense IR bands. Interestingly, the second of these bands shows a weak shoulder at its lower energy side.
- The very strong 1292 cm⁻¹ band is dominated by the $\nu(\text{CN})$ stretching vibration, coupled with some other motions [26]. In the case of magnesium acesulfamate, this band shows an important splitting into two components [13].
- The band related to the symmetric stretching mode, $\nu_{\text{s}}(\text{SO}_2)$, of the sulfonyl group, which is partially coupled with other vibration modes [26], is located practically at the same energy as in the case of the other alkaline-metal acesulfamates [10]. The corresponding anti-symmetric mode, $\nu_{\text{as}}(\text{SO}_2)$, appears at somewhat higher energy than in these cases [10].
- The very weak band at 425 cm⁻¹ was tentatively assigned to a ring mode, coupled with one of the water librational modes, $\rho_{\text{w}}(\text{H}_2\text{O})$, by comparison with the previous results obtained for magnesium acesulfamate [13].

Conclusions

We have synthesized and characterized the crystal structure and vibrational-spectroscopic properties of aqua lithium acesulfamate, Li(ace)H₂O the lightest member of the alkaline-metal family of acesulfamate salts.

Besides, condensing in a different crystal system as an aqua-acesulfamato complex, Li(ace)H₂O sharply departs from the other heavier alkaline-metal acesulfamates, namely M-ace (M: Na⁺, K⁺, Rb⁺, Cs⁺), which are members of a monoclinic isotypic family of salts.

The small lithium ionic radius limits the number of ligand atoms in its coordination sphere before ligand crowding takes place. In Li(ace)H₂O, lithium is in a distorted tetrahedral environment (LiO₄ core) which, at variance with the other analogue salts, does not include the deprotonated acesulfamate N-atom as a ligand.

There is a strong correlation of metal–ligand coordination distances with the metal ion radius in $\text{Li}(\text{ace})\text{H}_2\text{O}$ and along the isotypic M-ace (M: from Na^+ to Cs^+) series [$r(\text{Li}^+) < r(\text{Na}^+) < r(\text{K}^+) < r(\text{Rb}^+) < r(\text{Cs}^+)$]. In fact, M–O(carb) distances are 1.949(7) and 1.957(6) Å (Li), 2.345(2) and 2.352(2) Å (Na) and in the intervals 2.776–3.282 Å (K), 2.849(3)–3.432(4) Å (Rb), and 3.105(4)–3.396(5) Å (Cs); M–O(sulf) lengths are 1.943(7) Å (Li), 2.379(2) and 2.398(2) Å (Na) and in the ranges 2.724–3.053 Å (K), 2.882(3)–3.159(4) Å (Rb), and 3.054(5)–3.480(6) Å (Cs).

The $\text{Li}(\text{ace})\text{H}_2\text{O}$ solid is arranged in chains that extends along the crystal *a*-axis. These chains, in turn, are packed side-by-side conforming layers parallel to the crystal (*a*, *b*) plane. Adjacent layers are weakly bonded to each other through van der Waals interaction making (001) an easy-cleavage crystal plane.

Acknowledgements This work was supported by CONICET (PIP 11220130100651CO) and UNLP (Projects 11/X673 and 11/X709) of Argentina. OEP, GAE and BSP-C are Research Fellows of CONICET.

References

- Ager DJ, Pantaleone DP, Henderson SA, Katritzky AR, Prakash J, Walters DE (1998) Commercial synthetic nonnutritive sweeteners. *Angew Chem Int Edit* 37:869–876
- Kroger M, Meister K, Kava R (2006) Low-calorie sweeteners and other sugar substitutes: a review of the safety issues. *Compr Rev Food Sci Food Saf* 5:35–47
- Clauss K, Jensen H (1973) Oxathiazinone dioxides: a new group of sweetening agents. *Angew Chem Int Edit* 12:869–876
- Mayer DG, Kemper FH (eds) (1991) *Acesulfame-K*. Marcel Dekker, New York
- Paulus EF (1975) 6-Methyl-1,2,3-oxathiazin-4(3K)-on-2,2-dioxid. *Acta Crystallogr B* 31:1191–1193
- Baran EJ, Yilmaz V (2006) Metal complexes of saccharin. *Coord Chem Rev* 250:1980–1999
- Icbudak H, Adiyaman E, Uyanik A, Çakir S (2007) Synthesis, characterization and chromotropic properties of Mn^{II} , Co^{II} , Ni^{II} and Cu^{II} with bis(acesulfamato)bis(3-methylpyridine) complexes. *Transit Met Chem* 32:864–869
- Demirtas G, Dege N, Icbudak H, Yurdakul O, Büyükgüngör O (2012) Experimental and DFT studies on poly [d- μ_3 -acesulfamato-O,O,O',O':O,O-di- μ -acesulfamato-O–O,N-di- μ -aqua-dicalcium(II)] complex. *J Inorg Orgnomet Polym Mater* 22:671–679
- Piro OE, Echeverría GA, Parajón-Costa BS, Baran EJ (2014) Synthesis and characterization of ammonium acesulfamate. *Z Naturforsch* 69b:737–741
- Piro OE, Echeverría GA, Parajón-Costa BS, Baran EJ (2015) Structural and spectroscopic characterization of isotypic sodium, rubidium and cesium acesulfamates. *Z Naturforsch* 70b:491–496
- Baran EJ, Parajón-Costa BS, Echeverría GA, Piro OE (2015) Synthesis, structural and spectroscopic characterization of thallium(I) acesulfamate. *Maced J Chem Chem Eng* 34:95–100
- Icbudak H, Demirtas G, Dege N (2015) Experimental and theoretical (DFT) studies on poly [octa- μ_3 -acesulfamato-O,O,N,O':O',N:O,O-tetraaquabarium(II)] and poly [octa- μ_3 -acesulfamato-O,O,N,O':O',N:O,O-tetraaquastrontium(II)] complexes. *Maced J Chem Chem Eng* 34:105–114
- Piro OE, Echeverría GA, Parajón-Costa BS, Baran EJ (2016) Structural and IR-spectroscopic characterization of magnesium acesulfamate. *Z Naturforsch* 71b:51–55
- Deberitz J, Boche G (2003) Lithium und seine Verbindungen. *Chem unserer Zeit* 37:258–266
- Tarascon JM (2010) Is lithium the new gold? *Nat Chem* 2:510
- Baran EJ (ed) (2017) *Litio. Un recurso natural estratégico*. Academia Nacional de Ciencias Exactas, Físicas y Naturales, Buenos Aires
- Velaga SP, Vangala BP, Basavoju S, Boström D (2010) Polymorphism in acesulfame sweetener: structure-property and stability relationships of bending and brittle crystals. *Chem Commun* 46:3562–3564
- CrysAlisPro Software System (2009). Version 1.171.33.48 (release 15-09-2009-CrysAlis 171.NET), Oxford Diffraction Ltd., Abingdon, Oxford
- Sheldrick GM (2008) A short history of SHELX. *Acta Crystallogr A* 64:112–122
- Farrugia LJ (1997) ORTEP-3 for Windows: a version of ORTEP-III with a graphical user interface (GUI). *J Appl Crystallogr* 30:565
- Bach I, Kumberger H, Schmidbaur H (1990) Orotate complexes. Synthesis and crystal structure of lithium orotate (–) monohydrate and magnesium bis [orotate (–)] octahydrate. *Chem Ber* 123:2267–2671
- Tobón-Zapata GE, Piro OE, Etcheverry SB, Baran EJ (1998) Crystal structure and IR-spectrum of lithium citrate monohydrate, $\text{Li}(\text{C}_6\text{H}_7\text{O}_7) \cdot \text{H}_2\text{O}$. *Z Anorg Allg Chem* 624:721–724
- Wagner CC, Baran EJ, Piro OE, Castellano EE (1999) A new potentially useful complex for lithium therapies: dimeric monoaqua lithium isoorotate. *J Inorg Biochem* 77:209–213
- Mingos DMP (1998) *Essential trends in inorganic chemistry*. Oxford University Press, Oxford
- Yvon K, Jeitschko W, Parthe E (1977) LAZY PULVERIX, a computer program for calculating X-ray and neutron diffraction powder patterns. *J Appl Crystallogr* 10:73–74
- Popova AD, Velcheva EA, Stamboliyska BA (2012) DFT and experimental study on the IR spectra and structure of acesulfame sweetener. *J Mol Struct* 1009:23–29
- Siebert H (1966) *Anwendungen der Schwingungsspektroskopie in der Anorganischen Chemie*. Springer, Berlin
- Libowitzky E (1999) Correlation of O–H stretching frequencies and O–H...O hydrogen bond lengths in minerals. *Monatsh Chem* 130:1047–1059
- Smith B (1999) *Infrared spectral interpretation*. CRC Press, Boca Raton